DESIGN AND EXPERIMENTAL OPTIMIZATION OF AIRFOIL-TRIANGLE SIEVE FOR HAMMER MILL

/

锤片式粉碎机翼型三角形筛片设计与试验优化

Di Wang [1)], Changbin He [1)], Haiqing Wang [1)], Fei Liu [1)], Haiqing Tian*[1)], Liang Ma [2)] [1]

[1)] Inner Mongolia Agricultural University, College of Mechanical and Electrical Engineering, Hohhot/China;

[2)] Tuoketuo Senior Vocational Middle School, Hohhot/China

Tel: +86-0471-4309215; E-mail: hqtian@126.com

*DOI: https://doi.org/10.35633/inmateh-61-**3**4*

***Keywords:** Hammer mill, Airfoil-triangle sieve, Feed, Grinding, Experimental optimization*

ABSTRACT

The performance of a hammer mill is affected by the formation of a circulation layer. In this paper, an airfoil-triangle sieve was designed to destroy the circulation layer and improve the performance of the hammer mill. To determine the optimal design parameters of the airfoil-triangle sieve, three-factor and three-level tests were carried out by using the productivity and output per kW·h as the evaluation indexes and the airfoil camber, angle of attack and isosceles angle as the influencing factors. The order of the influences on the productivity was airfoil camber>angle of attack>isosceles angle. The order of the influences on the output per kW·h was angle of attack>airfoil camber>isosceles angle. The optimum combination after parameter optimization was determined to be as follows: airfoil camber of 0.15, angle of attack of 10° and isosceles angle of 113°. A test was carried out with to the optimum parameter combination. The results showed that the productivity and output per kW·h were 1101.56 kg/h and 188.97 kg/kW·h, respectively, which were consistent with the predicted results. The regression model was reliable.

摘要

针对锤片式粉碎机工作时物料环流层影响机器性能（生产率、功率消耗）的问题，本文以 CPS-420 型锤片式粉碎机为研究样机，设计了翼型三角形筛片，以破坏物料环流层，提高粉碎机性能。为确定筛片最佳设计参数，以翼型三角形筛片的弯度、冲角、等边角度数为试验因素，以生产率和度电产量为评价指标，利用 Box-Benhken 试验方法进行了三因素三水平响应面试验分析。结果表明：对生产率影响的主次因素为：弯度>冲角>等边角度数；对度电产量影响的主次因素为：冲角>弯度>等边角度数。基于响应面法进行参数优化，确定筛片设计最佳参数组合为弯度 0.15，冲角 10°，等腰角度数 113°。以优化后的参数组合进行试验验证，试验结果为：生产率和度电产量分别为 1101.56kg/h、188.97kg/kW·h，与模型预测结果基本吻合，回归模型可靠。

INTRODUCTION

Hammer mill is widely used in feed production because of their simple structure, good generality and convenient maintenance (*Zhang et al., 2019; Bochat et al., 2015; Nakamura et al., 2015; Polari et al., 2019*). However, in the working process of a hammer mill, a circulation layer easily forms in the grinding chamber. The existence of a circulation layer can lead to the problems of high energy consumption and excessive grinding of materials (*Cao, 2010; Wang et al., 2013; Wang et al., 2017; Qian et al., 2020*).

To solve this problem, many methods have been used to destroy the circulation layer and improve the performance of hammer mill. Changing the shape of the grinding chamber is a common method. Drip type grinding chambers are most commonly used in production because this type of chamber can constantly change the gap between the hammer and sieve to destroy the circulation layer and improve the performance of the hammer mill (*Cui et al., 2018*). In addition, some researchers have designed hexagonal and elliptical grinding chambers (*Qin, 2009*). A jet nozzle was added to the grinding chamber, and high-pressure gas was used to spray the circulation layer to destroy it. Research has shown that this method can improve the productivity and service life of hammer mill (*Kong et al., 2018*). Some researchers have also used vibrating sieves to destroy the circulation layer (*Chen et al., 2008*). Cao Liying (*Cao, 2010*) designed a new type of hammer mill, replacing the sieve in the grinding chamber with a truss plate and installing the sieve at the

[1] *Di Wang, Ph.D. Stud. Eng.; Changbin He, Lec. Ph.D. Eng.; Haiqing Wang, M.S. Eng.; Fei Liu, As. Prof. Ph.D. Eng.; Haiqing Tian, Prof. Ph.D. Eng.; Liang Ma, Eng.*

outlet, to eliminate the circulation layer in the grinding chamber. Although the above methods can improve the performance of hammer mill to a certain extent, these methods are difficult to realize.

Considering that it is easy to change the shape of the sieve, this paper aimed to destroy the circulation layer by designing a new type of sieve, and then improve the performance of the hammer mill. The structural parameters of a CPS-420-type hammer mill were referred, and an airfoil-triangle sieve was designed. The Box-Benhken test method was used to obtain the optimal parameter combination for the airfoil-triangle sieve. The research results provide a theoretical basis and reference for the optimal design of the hammer mill sieve.

MATERIALS AND METHODS

- **Test materials and equipment**

Corn grain was selected as the test material. The variety of corn used was JINSHAN-126, with a moisture content of 12.54% and bulk density of 723 kg/m^3. The test equipment included a TCS-150 type electronic scale (accuracy of 0.01 kg), a BT223S type electronic balance (accuracy of 0.001 g), an electric energy meter, a stopwatch and a drying box, etc.

- **Overall structure and working principle**

CPS-420 type hammer mill is mainly composed of a feeding hopper, a sieve, a hammer, an outlet, a frame, and a motor. The structure of the hammer is shown in Fig. 1, and the main specifications are given in Table 1.

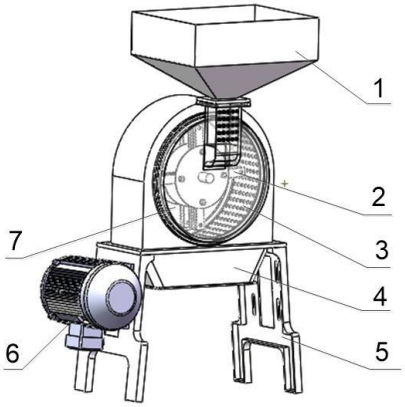

Fig. 1 – Overall structure of hammer mill

1 – Feeding hopper; 2 – Hammer; 3 – Sieve frame and sieve; 4 – Outlet; 5 – Frame; 6 – Motor; 7 – Grinding chamber

Table 1

Specification of hammer mill

Specification	Value
Motor power	3 kW
Rotational speed of rotor	4400 r/min
Number of hammers	24
Sieve width	180 mm
Size of the sieve holes	3 mm
Size (length × width × height)	850×800×1300 mm

When the hammer mill is working, the corn materials enter the grinding chamber through the feed hopper and are broken down by the high-speed rotating hammer. After that, the materials collide with the sieve at a higher speed and are further broken down. The particles that are small enough enter the outlet through the sieve holes, and the large particles continue to be ground until the particle size is smaller than the sieve hole diameter.

- **Design of the airfoil-triangle sieve**

The design requirements of the airfoil-triangle sieve should meet the installation size of the sieve frame and support a simple manufacturing process. Additionally, the airfoil-triangle sieve should be able to destroy the circulation layer and improve the performance of the hammer mill.

The design principle of the airfoil-triangle sieve is shown in Fig. 2. Considering the uniform stress on the sieve, the sieve was evenly divided into four equal parts along the circumference, each of which was composed of the airfoil arc, arc and isosceles angle. The circumference line (D=400 mm) is formed by connecting the vertices of each isosceles angle in each equal part and is concentric with the arc (d=380 mm). Additionally, the diameters D and d are the installation size of the sieve on the sieve frame and represent the inner diameter and outer diameter of the groove of the sieve frame, respectively. The airfoil arc is composed of arcs with radii of R_1 and R_2. The centres of the two arcs are determined by points a, b and c. Points a and b are the contact points between the airfoil arc and arc of diameter d and depend on the central angle δ of the airfoil arc. Point c is the highest chord point of the airfoil arc according to the airfoil design theory (*Du., 2015*), which is located at 1/4 of the chord length of the airfoil arc (from point a to b). The value of the isosceles angle is θ, which is located in the middle of each equal part. The equations for R_1 and R_2 can be obtained from Fig. 2.

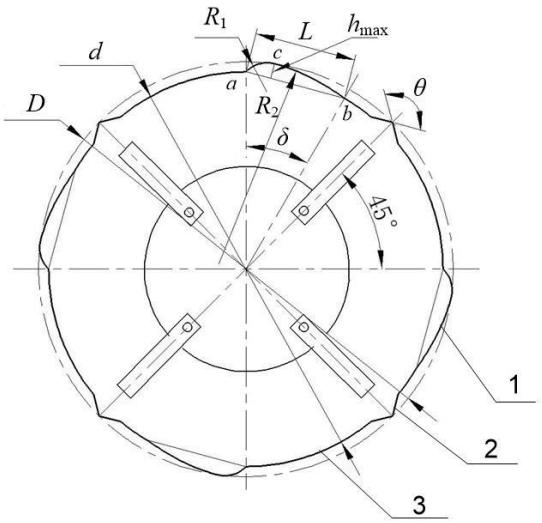

Fig. 2 – Design principle diagram of airfoil-triangle sieve
1 – Airfoil arc 2 – Isosceles angle 3 – Arc

$$R_1 = \frac{h_{\max}^2 + (\frac{L}{4})^2}{2h_{\max}} \quad (1)$$

$$R_2 = kf \quad (2)$$

$$f = \frac{h_{\max}}{L} \quad (3)$$

$$L = d\sin\frac{\delta}{2} \quad (4)$$

Where:

$h_{\max}$ is maximum chord height of the airfoil arc, [mm];

L is chord length of the airfoil arc, [mm];

f is the airfoil camber, which is determined by the installation size of the sieve.

In this paper, the range of f is 0.1-0.15; k is the radius coefficient, which is derived from the geometric relationship between radius R_2 and chord ab; and the range is 1000-2000.

In the area of the airfoil arc, the air flow has a great influence on the material sieving efficiency, and the air flow is related to the angle of attack.

As shown in Fig. 3 (n is the rotor speed, r/min, and v_s is the air flow velocity, m/s), the angle of attack τ is the angle between the chord of the airfoil arc and the air flow direction, and the geometric relationship shows that $\delta=2\tau$; previous research showed that when the angle of attack was in the range of 3-15° (*Du., 2015*), the sieving efficiency of the material was the best.

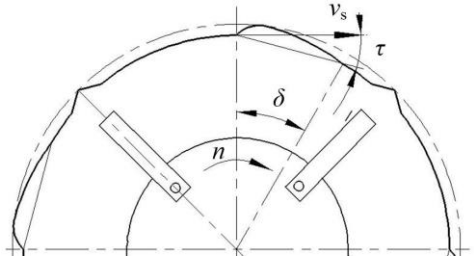

Fig. 3 – Schematic diagram of the angle of attack

A physical picture of the airfoil-triangle sieve is shown in Fig. 4.

Fig. 4 – Airfoil-triangle sieve

- **Theoretical analysis of the installation of an airfoil-triangle sieve in a hammer mill**

As shown in Fig. 5, when the hammer moves to the nearest distance from the sieve, the gap between the hammer and sieve is very small, and the circulation layer forms a reduced air flow jet through this area. Additionally, the high-speed rotation of the rotor produces a radial centrifugal force, which produces radial air flow. The reduced air flow jet collides with the radial air flow to form vortices. This vertical motion destroys the circulation layer and increases the probability that the hammer hits the material. In addition, the movement of multiple vortices continue to consume energy, thus reducing the speed of materials, resulting in a larger relative speed between materials and hammers and improving the grinding efficiency.

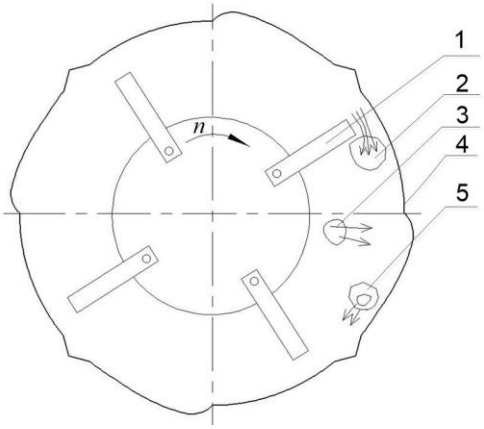

Fig. 5 – Schematic diagram of flow field motion analysis in an airfoil-triangle sieve

1-Hammer; 2-Reduced air flow jet; 3-Radial air flow; 4-Airfoil-triangle sieve; 5-Vortex

- **Experimental design**

Previous research has shown that the airfoil camber, angle of attack and isosceles angle of the airfoil-triangle sieve have a great influence on the performance of hammer mill. According to the structural parameters of the sieve frame and the above analysis data, the range of the airfoil camber is 0.1-0.15, the range of the angle of attack is 9-15°, and the range of the isosceles angle is 90-150°. The Box-Benhken test scheme was used to investigate three factors and three levels of test research. Each group of tests was repeated three times, and the average value of the test results was taken. The test factors and levels are shown in Table 2.

Table 2

Experimental factors and levels

Levels	Airfoil camber A	Angle of attack B	Isosceles angle C
	/	[°]	[°]
-1	0.1	9	90
0	0.125	12	120
1	0.15	15	150

- **Performance evaluation of hammer mill**

According to the Chinese national standard GB/T 6971-2007, the productivity and output per kW·h were taken as the performance evaluation indexes of the hammer mill. The calculation formulas are given by formulas (5) and (6) (*China National Standardization Committee, 2007*).

$$E_c = \frac{Q_c}{T_c} \tag{5}$$

where E_c is the productivity of the hammer mill, kg/h; Q_c is the mass of the fragmented test sample, kg; and T_c is the duration of grinding of a single test sample, h.

$$G = \frac{Q_c}{G_n} \tag{6}$$

where G is the output per kW·h of the hammer mill, kg/kW·h; and G_n is the power consumption during grinding of a single test sample, kW·h.

RESULTS

- **Test results and analysis**

According to the test scheme, 17 groups of tests were performed, and each group of tests was repeated three times. The average values were taken as the test results, and the indexes were calculated according to formulas (5) and (6). The test results are shown in Table 3.

Table 3

The test results

Test number	Airfoil camber A	Angle of attack B	Isosceles angle C	Productivity	Output per kW·h
	/	[°]	[°]	[kg/h]	[kg/kW·h]
1	-1	1	0	1059.24	178.49
2	0	-1	1	1054.92	183.47
3	0	1	1	1048.66	177.23
4	-1	-1	0	1058.52	184.31
5	0	-1	-1	1062.26	187.91
6	1	0	1	1086.34	187.62
7	0	0	0	1081.46	185.16
8	1	0	-1	1103.16	186.12
9	0	1	-1	1045.4	179.14
10	1	1	0	1082.52	185.28
11	0	0	0	1084.12	185.63
12	-1	0	1	1068.28	178.25
13	-1	0	-1	1061.24	183.37
14	1	-1	0	1100.86	194.57
15	0	0	0	1085.9	186.91
16	0	0	0	1086.42	184.35
17	0	0	0	1082.76	185.29

Analysis of variance and the regression model

The test results were analysed by Design-Export 10 software, and the results are presented in Table 4. The regression models of E_c and G were obtained as formulas (7) and (8). From the analysis of variance, we can see that the two models were extremely significant ($P<0.01$), and the lack of fit was not significant ($P>0.05$). The fitting coefficients R^2 of model 1 and model 2 were 0.9941 and 0.9745, respectively, which

showed that the correlation between the predicted and actual values was high, and the test error was small. Through the analysis of variance, it can be concluded that the order of the influences on the productivity was airfoil camber A>angle of attack B>isosceles angle C, and there was extreme significance between each factor. From Table 4, the order of the influences on the output per kW·h was angle of attack B>airfoil camber A>isosceles angle C, and the AC interaction item had a significant influence on the output per kW·h.

$$E_c = 1084.13 + 15.70A - 5.09B - 1.73C - 4.77AB - 5.97AC + 2.65BC + 9.05A^2 - 17.90B^2 - 13.43C^2 \quad (7)$$

$$G = 185.47 + 13.65 - 3.76B - 1.25C - 0.87AB + 1.66AC + 0.63BC + 1.05A^2 - 0.85B^2 - 2.68C^2 \quad (8)$$

where A is the airfoil camber; B is the angle of attack, °; and C is the isosceles angle, °.

Table 4

The results of variance analysis

Source	DF	MS	F Value	P Value	Source	DF	MS	F Value	P Value
Model 1	9	545.67	130.80	< 0.0001**	**Model 2**	9	31.69	29.76	< 0.0001**
A	1	1971.92	472.69	< 0.0001**	**A**	1	106.36	99.90	< 0.0001**
B	1	207.47	49.73	0.0002**	**B**	1	113.40	106.51	< 0.0001**
C	1	24.01	5.76	0.0475*	**C**	1	12.43	11.67	0.0112*
AB	1	90.82	21.77	0.0023**	**AB**	1	3.01	2.83	0.1366
AC	1	142.32	34.12	0.0006**	**AC**	1	10.96	10.29	0.0149*
BC	1	28.09	6.73	0.0357*	**BC**	1	1.60	1.50	0.2599
A^2	1	344.78	82.65	< 0.0001**	**A^2**	1	4.63	4.35	0.0755
B^2	1	1348.49	323.25	< 0.0001**	**B^2**	1	3.07	2.88	0.1333
C^2	1	758.98	181.94	< 0.0001**	**C^2**	1	30.16	28.33	0.0011**
Lack of Fit	3	3.94	0.91	0.5126	**Lack of Fit**	3	1.32	1.52	0.3385
Pure Error	4	4.35			**Pure Error**	4	0.87		
Cor Total	16				**Cor Total**	16			

*Note: P < 0.01 (extremely significant, **), P < 0.05 (significant, *);*
Model 1 is variance analysis of productivity.
Model 2 is variance analysis of output per kW·h.

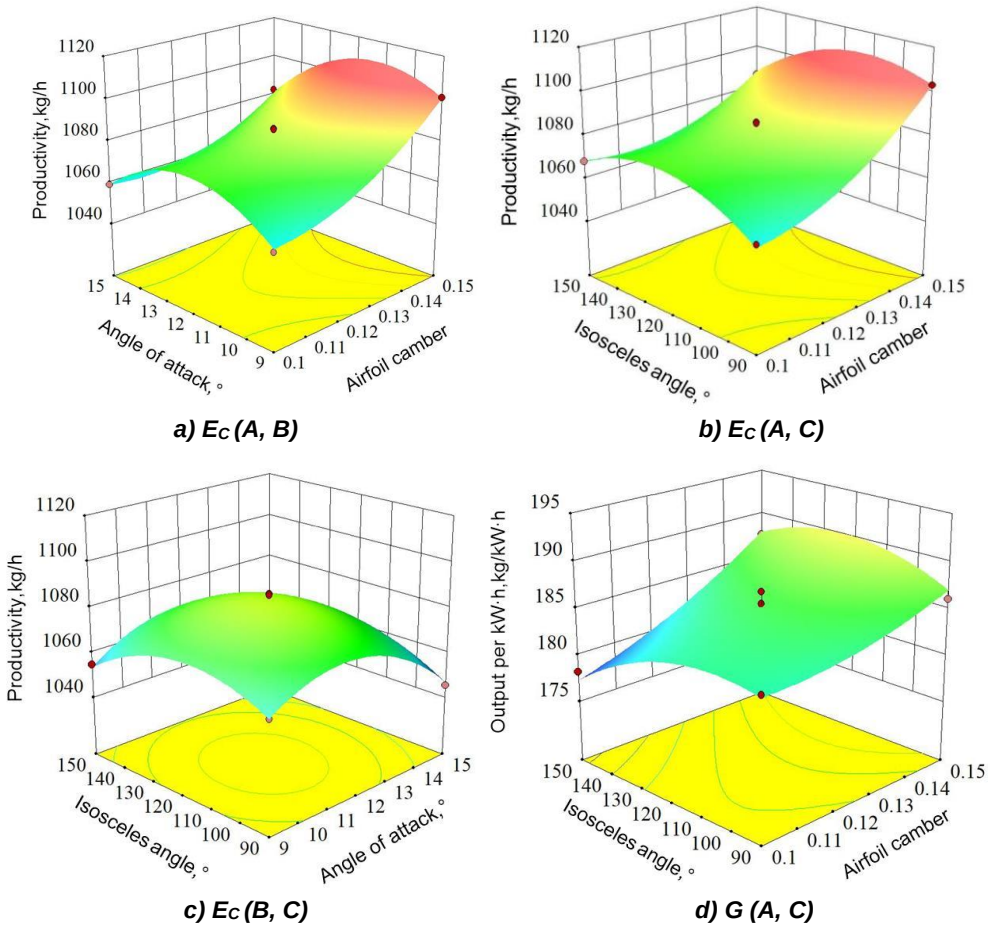

a) E_C (A, B) *b) E_C (A, C)*

c) E_C (B, C) *d) G (A, C)*

Fig. 6 – Response surface results

- **Analysis of the influences of the interaction factors on productivity**

The response surfaces of the airfoil camber, angle of attack and isosceles angle with productivity are shown in Fig. 6a-6c. When the isosceles angle was 120°, the productivity increased with increasing airfoil camber. With increasing impact angle, the productivity first increased and then decreased (Fig. 6a). When the angle of attack was 12°, the productivity increased slowly with increasing isosceles angle (Fig. 6b). When the airfoil camber was 0.125, with increasing isosceles angle and impact angle, the production first increased and then decreased (Fig. 6c).

The overall influence trend was that the productivity was high when the angle of attack and isosceles angle were moderate and the airfoil camber was large. The main reasons for these results are as follows: When the airfoil camber increases, the intensity of the vortices in the area of the airfoil arc increases. These vortices continuously turn the material over, and the probability of the material being hit by the hammer is increased, improving the grinding efficiency of the material and improving the productivity of the hammer mill. The isosceles angle affects the angle of the material impacting the sieve. When the isosceles angle is very large or small, the material and sieve do not have an ideal impact angle, thus reducing the efficiency of the material sieving and further reducing the productivity of the hammer. When the angle of attack is small, the air flow has less effect on the material. When the impact angle is large, the air flow resistance coefficient becomes larger, which hinders the material sieving and reduces the productivity of the hammer.

- **Analysis of the influence of the interaction factors on the output per kW·h**

The response surface of the isosceles angle and airfoil camber with the output per kW·h is shown in Fig. 6d. When the angle of attack was 12°, the output per kW·h first increased slowly and then decreased with increasing isosceles angle. The change in the output per kW·h was very small with increasing airfoil camber.

The overall influence trend was that the output per kW·h was high when the isosceles angle was moderate. This occurs because when the isosceles angle is large or small, the impact angle between the material and sieve is not ideal. The sieving efficiency is reduced, material particles are excessively ground, and the electric energy consumption of hammer increases.

- **Parameter optimization and validation**

To obtain the optimal design parameters of the airfoil-triangle sieve, the regression equation was further solved by using Design-Export 10 software (*Wang et al., 2019*; *Du et al., 2019*). The objective function and constraints are as follows:

$$\begin{cases} \max E_C \\ \max G \\ A \in [0.1-0.15] \\ B \in [9°-15°] \\ C \in [90°-150°] \end{cases} \quad (7)$$

From the optimization, the optimum parameter combination of the airfoil-triangle sieve was obtained as follows: airfoil camber of 0.15, angle of attack of 10° and isosceles angle of 113°. The predicted values of the productivity and output per kW·h were 1109.62 kg/h and 192.54 kg/kW·h, respectively.

To verify the reliability of the predicted values, a validation test was carried out, and the test results were as follows: the productivity was 1101.56 kg/h, and the output per kW·h was 188.97 kg/kW·h. The prediction error was less than 2%, which showed that the prediction model of this study was reliable.

CONCLUSIONS

1. In this paper, an airfoil-triangle sieve was innovatively designed. It was verified that the airfoil-triangle sieve could destroy the circulation layer and improve the performance of the hammer mill.

2. The regression models of the productivity and output per kW·h were established, and the primary and secondary factors affecting the performance indexes of the hammer mill were obtained. The results showed that the order of the influences on the productivity was airfoil camber>angle of attack>isosceles angle, and the order of the influences on the output per kW·h was angle of attack>airfoil camber>isosceles angle.

3. The optimum combination after parameter optimization was determined to be as follows: airfoil camber of 0.15, angle of attack of 10° and isosceles angle of 113°. A test was carried out according to the optimum parameter combination. The results showed that the productivity and output per kW·h were 1101.56 kg/h and 188.97 kg/kW·h, respectively. This was consistent with the optimization results, and thus, the regression model was reliable.

ACKNOWLEDGEMENTS

This project was funded by the National Natural Science Foundation of China (NSFC) (No. 51765055) and the Inner Mongolia Special Project for Transformation of Scientific and Technological Achievements (No. 2019CG034).

REFERENCES

[1] Bochat A, Wesolowski L, Zastempowski M, (2015), A Comparative Study of New and Traditional Designs of a Hammer Mill, *Transactions of the ASABE*, Vol. 58, Issue 3, pp.585-596, MI/USA;

[2] Cao Liying, (2010), *Measuring and Simulating Analysis on Material-Sieving Properties for a New Hammer Mill* (新型锤片式粉碎机分离特性的模拟与测试分析), PhD dissertation, Inner Mongolia Agricultural University, Hohhot/China;

[3] Chen Weixu, Ma Jun, Shen Chengjun, (2008), Experimental research on the SZF-11 pulveriser (SZFS-11 粉碎机的试验研究), *Journal of Agricultural Mechanization Research*, Vol.30, Issue 12, pp. 134-135, Harbin/China;

[4] Du Jianan, (2015), *The design and experimental study on airfoil sieve crushing chamber of hammer mill* (锤片式粉碎机翼形筛片的设计与试验研究), MSc dissertation, Inner Mongolia Agricultural University, Hohhot/China;

[5] Kong Tenghua, Gong Guifen, (2018), Optimization design of the crushing chamber of the hammer mill (锤片式粉碎机粉碎室的优化设计), *Feed Research*, Vol.41, Issue 1, pp.47-52, Beijing/China;

[6] Nakamura H, Kan H, Takeuchi H, et al, (2015), Effect of stator geometry of impact pulveriser on its grinding performance, *Chemical Engineering Science*, Vol.122, pp.565-572, England/UK;

[7] Polari J. J., Wang S. C., (2019). Hammer mill sieve design impacts olive oil minor component composition, *European Journal of Lipid Science and Technology*, Vol. 121, Issue 10, DOI:10.1002/ejlt.201900168, Weinheim/GERMANY;

[8] Qian Yi, Wang Di, Zhang Jue, et al, (2020), Numerical simulation and experimental research on gas flow field of special-shaped sieve sheet of crusher (粉碎机异形筛片气流场数值模拟及试验研究), *Journal of China Agricultural University*, Vol.25, Issue 3, pp. 79-87, Beijing/China;

[9] Qin Yonglin, (2009), *Studies on the Effects of Hammer Mill Performance on the Grinding Results of Normal Feedstuffs* (锤片式粉碎机性能对常规饲料粉碎效果影响), MSc dissertation, Jiangnan University, Wuxi/China;

[10] Cui Xiangquan, Li Hansong, He Xiaodong, et al, (2018), The designing of the pulveriser with the water drop-shaped teeth-claw model No.FSSP8020 (FSSP8020 型水滴形齿爪粉碎机的设计), *Feed Industry*, Vol.39, Issue 15, pp. 11–13, Shenyang/China;

[11] Wang Weiguo, Yu Xinguo, Yu Zheng, (2017), Latest advancement in technology innovation of fine grinding hammer mill (锤片式微粉碎机技术创新的最新进展), *Feed Industry*, Vol.38, Issue 13, pp.1-4, Shenyang/China;

[12] Wang Jianxin, Zhang Guangyi, Cao Liying, (2013), Research of materials motion law in separation flow of new type hammer feed grinder (新型锤片式饲料粉碎机分离流道内物料运动规律). *Transactions of the Chinese Society of Agricultural Engineering*, Vol.29, Issue 9, pp. 18-23, Beijing/China;

[13] Wang Shengsheng, Ji Jiangtao, Jin Xin, et al, (2019), Design and experimental optimization of cleaning system for peanut harvester, *INMATEH-Agricultural Engineering*, Vol. 57, Issue 1, pp.243-252, Bucharest/Romania;

[14] Xiaobin Du, Junlin He, Yongqiang He, et al, (2019), Parameter Optimisation and Experiment on the Combing of Cerasus Humilis, *INMATEH-Agricultural Engineering*, Vol. 57, Issue 1, pp.103-114, Bucharest/Romania;

[15] Zhang Yongjie, Xu Hongmei, Liu Shuang, et al, (2019), Finite element analysis and topology optimization of hammer feed grinder frame plate (锤片式饲料粉碎机架板的有限元分析及拓扑优化), *Journal of Huazhong Agricultural University*, Vol.38, Issue 4, pp.1-5, Wuhan/China;

[16] ***China Agricultural Machinery Standardization Technical Committee, (2007), Test method for feed mill, *GB/T6971-2007*, Standards Press of China, Beijing/China.